Dalton Transactions

ROYAL SOCIETY OF CHEMISTRY

PAPER

View Article Online
View Journal | View Issue

Cite this: *Dalton Trans.*, 2024, **53**, 11884

Activation and functionalisation of carbon dioxide by bis-tris(pyrazolyl)borate-supported divalent samarium and trivalent lanthanide silylamide complexes†

Tajrian Chowdhury, Claire Wilson and Joy H. Farnaby *

Received 10th May 2024,
Accepted 18th June 2024

DOI: 10.1039/d4dt01382d

rsc.li/dalton

Synthesis and reactivity with carbon dioxide (CO_2) of divalent samarium in the bis-tris(pyrazolyl)borate ligand environment has been reported. In addition, CO_2 activation and functionalisation by lanthanide silylamides in the bis-tris(pyrazolyl)borate ligand environment was demonstrated. Reduction of the Sm(III) precursor [Sm(Tp)$_2$(OTf)] (Tp = hydrotris(1-pyrazolyl)borate; OTf = triflate) with KC_8 yielded the insoluble Sm(II) multi-metallic coordination polymer [{Sm(Tp)$_2$}$_n$] **1-Sm**. Addition of 1,2-dimethoxyethane (DME) to **1-Sm** enabled isolation of the monomeric complex [Sm(Tp)$_2$(DME)] **1-Sm(DME)**. Complex **1-Sm(DME)** reduced CO_2 to yield the oxalate-bridged dimeric Sm(III) complex [{Sm(Tp)$_2$}$_2$(μ-η^2:η^2-O$_2$CCO$_2$)] **2-Sm**. The reactions of heteroleptic Ln(III) silylamide complexes [Ln(Tp)$_2$(N″)] (Ln = Y, Sm; N″ = N(SiMe$_3$)$_2$) with CO_2 yielded monomeric Ln(III) silyloxides [Ln(Tp)$_2$(OSiMe$_3$)] **3-Ln** and trimethylsilyl isocyanate (O=C=NSiMe$_3$). Complexes **3-Ln** are the first crystallographically characterised examples of Ln(III)–OSiMe$_3$ bonds accessed *via* CO_2 activation and functionalisation. Full characterisation data are presented for all complexes, including solid-state molecular structure determination by single-crystal X-ray diffraction.

Introduction

Carbon dioxide (CO_2) activation and functionalisation by complexes of transition metals (TM),[1] rare-earth metals lanthanides (Ln, where Ln = Sc, Y, La–Lu) and actinides,[2] and heterobimetallic systems,[3] have attracted significant interest from scientific communities worldwide, since CO_2 is the largest single source contributor to the greenhouse effect and climate change. CO_2 is a renewable one-carbon (C_1) building block and can bind to metal ions in various ways during activation,[4] which upon functionalisation yields valuable synthetic products and commercially important chemicals.[5]

Divalent Sm(II) ion, which is a powerful one electron reductant,[6] can activate CO_2 to yield oxos (O^{2-}), oxalates ($C_2O_4^{2-}$), and carbonates (CO_3^{2-}), the mechanism of which is well-modelled by computational methods (Fig. 1(a)).[7] For Sm(II) in an organometallic ligand environment, the first step of CO_2 activation at a Sm(II) metal centre involves the cooperative double reduction of CO_2 to CO_2^{2-} by two Sm(II) ions to form a reactive bimetallic intermediate [Sm]–(μ-η^2:η^1-CO$_2$)–[Sm] ([Sm] = Sm^{III}). This intermediate further reacts in two possible ways, where either (i) reaction with another molecule of CO_2 induces a C–C coupling reaction to form an oxalate-bridged dimeric complex [Sm]–(μ-η^2:η^2-O$_2$CCO$_2$)–[Sm] (Fig. 1(a)(i)) or (ii) where it loses a CO molecule and the resultant bimetallic oxo complex [Sm]–(μ-O)–[Sm] reacts with a free CO_2 molecule to form a bimetallic carbonate complex [Sm]–(μ-CO$_3$)–[Sm] (Fig. 1(a)(ii)).[7c] In the activation of CO_2 by [Sm(Cp*)$_2$(THF)$_2$] (Cp* = C$_5$Me$_5$), pathway (i) from Fig. 1(a) was shown to be the predominant pathway both experimentally and computationally,[7c] and any radical dimerization pathways have been deemed unlikely at the Sm(II) metal centre.[7] Outcome of the reactivity of CO_2 with low valent rare-earth metals is challenging to predict from first principles. The selectivity of CO_2 activation reactions of Sm(II) to yield oxalates *vs.* carbonates, can sometimes be rationalised based on the steric influence of the ancillary ligands of the Sm(II) ion, for example the more sterically bulky organometallic cyclopentadienyl ligand derivatives and macrocyclic ligands result in formation of carbonates.[7f,h] For trivalent U(III) it was shown that tuning the steric bulk of the ancillary cyclopentadienyl ligand (more sterically bulky ancillary ligands favoured the formation of carbonates over oxalates)[8] or where utilising different reaction temperatures led to the isolation of the thermodynamic (carbonate) *vs.* kinetic (oxalate) products.[9]

School of Chemistry, Joseph Black Building, University of Glasgow, Glasgow, G12 8QQ, UK. E-mail: Joy.Farnaby@glasgow.ac.uk

† Electronic supplementary information (ESI) available. CCDC 2347954–2347960. For ESI and crystallographic data in CIF or other electronic format see DOI: https://doi.org/10.1039/d4dt01382d

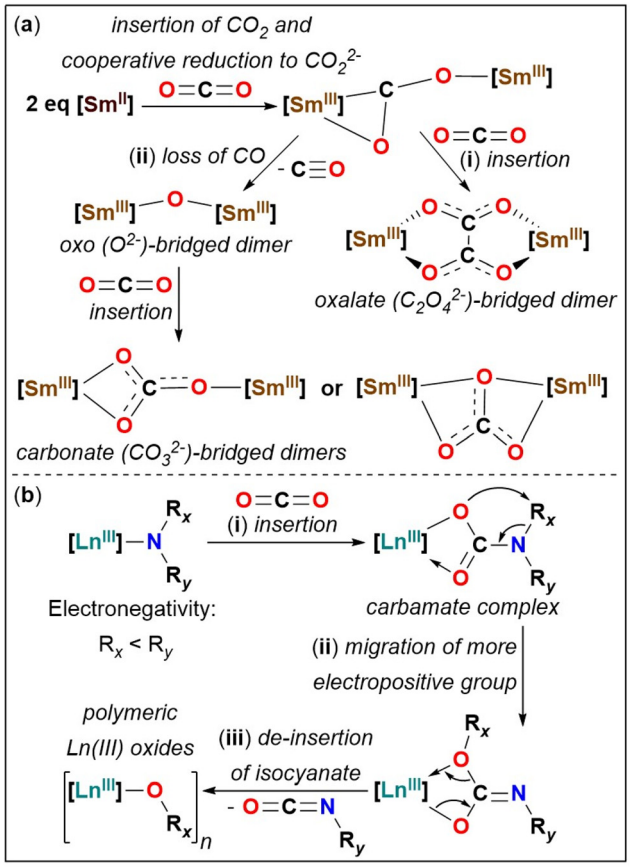

Fig. 1 Mechanistic pathway of CO_2 activation and functionalisation by (a) Sm(II)[7c] and (b) Ln(III)-amides.[10b]

Lewis acidic lanthanides activate CO_2 in various ways such as (a) the insertion of CO_2 into Ln(III)–X σ-bonds (X = amide, alkyl, alkyl/aryloxy, hydride, chalcogenide, carbene)[2a] and (b) cooperative reduction of CO_2 by Ln(II).[7a,c,e] Since Ln–N(amide) bonds exhibit remarkable substrate insertion scope[10] and catalytic activity,[11] the homoleptic Ln(III) silylamides [Ln(N″)$_3$] (N″ = N(SiMe$_3$)$_2$)[12] have been studied for small-molecule activation.[2a,13] The activation and functionalisation of CO_2 at the Ln(III) metal centre of a Ln–N(amide) bond proceeds *via* three steps. As shown in Fig. 1(b), these are: (i) insertion of CO_2 into [Ln]–NR$_2$ σ-bonds to form a carbamate complex [Ln]–(κ^2-O,OCNR$_2$) (Fig. 1(b)(i)), (ii) migration of the more electropositive amide substituent from the nitrogen atom to the oxygen atom within the carbamate complex (Fig. 1(b)(ii)), and (iii) de-insertion of isocyanate to yield Ln(III) oxides (Fig. 1(b)(iii)).[2a,10b] Isolation of carbamate complexes has proven challenging in the reactivity of CO_2 with [Ln(N″)$_3$], owing to the facile thermodynamic migration of the SiMe$_3$ group (as in (ii)), leading to the formation of insoluble polymeric Ln(III) silyloxides [{Ln(OSiMe$_3$)$_3$}$_n$].[2a,10b,14] Therefore, in absence of isolation of discrete Ln(III) silyloxides, CO_2 activation by Ln–N″ bonds have been exclusively studied by isolating the corresponding organic products: O=C=NSiMe$_3$, (Me$_3$Si)$_2$O, Me$_3$SiN=C=NSiMe$_3$, analogous to main-group metal–N″ mediated CO_2 activation.[2a,10b,15] Ln(III) silyloxides are potential precursors towards silicate materials and catalysts for organic transformations.[14b] Various synthetic routes to access Ln–OSiR$_3$ bonds exist, however insertion of CO_2 into Ln–N(amide) bonds to access molecular Ln(III) silyloxides remains a rare route.[14b,16]

Trofimenko's tridentate scorpionate N-donor hydrotris(1-pyrazolyl)borate (Tp) ligand and its derivatives (Tp^R) are robust ancillary ligands in Ln chemistry, which provide great structural diversity to Ln complexes and result in useful physical (optical, magnetic) and chemical (small-molecule activation, catalysis) properties.[17] The Sm(II) complexes [Sm(Tp^R)$_2$] display activation of a wide range of small-molecules (CO,[18] NO,[19] O$_2$,[20] S$_8$,[21] dichalcogenides,[22] azobenzene,[23] aldehyde,[24] ketones,[24,25] quinones,[24,25] azines[24]). Reduction of heavy-metal (Hg(I), Tl(I)) salts with [Sm(Tp*)$_2$] (Tp* = hydrotris(3,5-dimethyl-1-pyrazolyl)borate) was utilised to synthesise organometallic complexes: (a) the first Tp/cyclopentadienyl-mixed complex of a lanthanide[26] and (b) an alkynide.[27] Reactions of [Sm(Tp*)$_2$] with TM carbonyl complexes enabled isolation of heterometallic TM/Sm complexes.[28] The synthetic routes to [Ln(Tp^R)$_2$] complexes, with one exception,[29] have predominantly relied on Ln(II) precursors.[17a,23,29,30] Reduction of Ln(III) [Ln(Tp)$_2$(OTf)] (OTf = triflate) was shown as a viable route to access Ln(II) [Ln(Tp)$_2$] (Ln = Eu, Yb) complexes.[31] Utilising two small unsubstituted Tp ligands enabled isolation of the reactive Ln(III) amide complexes [Ln(Tp)$_2$(N″)],[32] which were inaccessible in the bulky [Ln(Tp*)$_2$]$^+$ ligand environment.[33]

Here we report the reduction of [Sm(Tp)$_2$(OTf)],[32c] to the Sm(II) complex [Sm(Tp)$_2$(DME)] **1-Sm(DME)**. The reactivity of **1-Sm(DME)** with small-molecules such as pnictogens and CO_2 has been investigated. Furthermore, the activation and functionalisation of CO_2 by the bis-Tp Ln(III) amide complexes [Ln(Tp)$_2$(N″)] (Ln = Y, Sm) has been reported.

Results and discussion

Synthesis of [Sm(Tp)$_2$(DME)] 1-Sm(DME)

The formal reduction potential (E^0) of Sm^{3+}/Sm^{2+} (−1.55 V) in aqueous solution *vs.* the Normal Hydrogen Electrode (NHE) makes it the most accessible classical Ln(III) candidate for reduction after Ln = Eu (−0.35 V) and Yb (−1.15 V).[34] Recently, the synthesis of soluble adduct-free Ln(II) [Ln(Tp)$_2$] (Ln = Eu, Yb) complexes was reported by reduction of Ln(III) [Ln(Tp)$_2$(OTf)] (OTf = triflate) with KC$_8$ in toluene.[31] However, in pursuit of non-classical Ln(II) ions,[35] as investigated herein, the bis-Tp ligand environment has been shown to be unsuccessful in stabilising non-classical Ln(II) ions. For example, the reaction between Ln(III) [Ln(Tp)$_2$(OTf)] (Ln = Y,[32a] Dy[32b]) and KC$_8$ yielded complicated reaction mixtures containing [Ln(Tp)$_3$][32b,36] and this was observed irrespective of reaction conditions and solvent choices (see ESI section A3† for NMR data for the reaction of [Dy(Tp)$_2$(OTf)] with KC$_8$ in toluene). Additionally for Ln = Y, fragmentation of the Tp ligand was observed resulting in formation of [Y(Tp)$_2$(κ^2-pz)] (pz = pyrazolyl).

Such fragmentation of the Tp ligand by cleavage of a B–N bond, in the absence of a metal-based reduction, often leading to the isolation of pz-bound byproducts, has been observed in rare-earth Tp/Tp^{R} chemistry.[33,36c,37] Purification of [Y(Tp)$_2$(κ^2-pz)] away from complicated reaction mixtures containing [Y(Tp)$_3$] proved challenging, however, single-crystals were isolated on one occasion (see ESI section A1.3† for NMR data for [Y(Tp)$_2$(κ^2-pz)] and Fig. S65† for the molecular structure of [Y(Tp)$_2$(κ^2-pz)]).

Reduction of the Sm(III) triflate complex [Sm(Tp)$_2$(OTf)][32c] in toluene yielded highly insoluble dark brown solids, precluding isolation of a molecular complex. However, the reduction of [Sm(Tp)$_2$(OTf)] in THF under ambient conditions, resulted in a dark red-brown solution containing the Sm(II) complex [Sm(Tp)$_2$(THF)$_2$] **1-Sm(THF)** (Scheme 1). The reaction mixture was filtered to exclude excess KC_8 and graphite. THF was removed *in vacuo* and the dark red-brown solids were extracted into toluene. Filtration of the dark orange-brown suspension to exclude K(OTf) and removal of toluene *in vacuo* (10^{-2} mbar) from the extract led to desolvation of THF from **1-Sm(THF)** (observed on the NMR-scale) and isolation of the insoluble dark-brown multi-metallic coordination polymer [{Sm(Tp)$_2$}$_n$] **1-Sm** (91%, Scheme 1).

Since the solid-state molecular structure of [{Eu(Tp)$_2$}$_2$] exhibits two bridging μ-κ^1:η^5 Tp ligands,[31] it is anticipated that **1-Sm** can adopt similar extended bridging modes of the Tp ligand leading to insolubility of polymeric **1-Sm**, owing to the slightly larger ionic radius of Sm(II) compared to Eu(II).[38] In order to isolate a molecular complex of **1-Sm**, after removal of toluene in the synthesis, excess DME (1,2-dimethoxyethane) was added resulting in the formation of the DME-adduct complex [Sm(Tp)$_2$(DME)] **1-Sm(DME)**. Since **1-Sm(DME)** does not undergo desolvation upon application of vacuum (10^{-2} mbar), drying *in vacuo* led to the isolation of **1-Sm(DME)** (89%, Scheme 1). Complex **1-Sm(DME)** has excellent solubilities in coordinating (THF) and non-coordinating (benzene, toluene) solvents, but poor solubilities in hydrocarbon solvents (hexane). Elemental analysis of **1-Sm(DME)** is consistent with the [Sm(Tp)$_2$(DME)] formulation. Desolvation of Lewis base adducts from **1-Sm(LB)** (LB = THF, DME) is observed in solution of non-coordinating aromatic solvents slowly over time (LB = THF, 2 days; DME, 2 weeks) under ambient conditions or quickly with heating (1 hour in both cases), leading to liberation of free Lewis bases and formation of insoluble **1-Sm** and [Sm(Tp)$_3$].[36b]

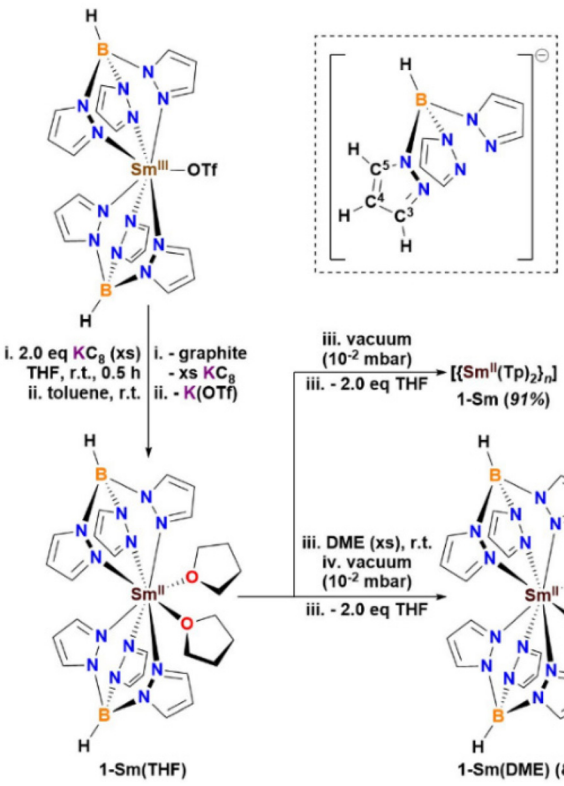

Scheme 1 Synthesis of Sm(II) [Sm(Tp)$_2$(DME)] **1-Sm(DME)** *via* [Sm(Tp)$_2$(THF)$_2$] **1-Sm(THF)** by reduction of [Sm(Tp)$_2$(OTf)] with KC_8 in THF and DME complexation to [{Sm(Tp)$_2$}$_n$] **1-Sm**. Note: The box shows numbering of the pyrazolyl carbon atoms of the Tp ligand.

Spectroscopy of [Sm(Tp)$_2$(DME)] 1-Sm(DME)

By relative integration, in the ^{1}H NMR spectrum of paramagnetic **1-Sm(DME)** in d_8-THF, the Tp-pyrazolyl protons in **1-Sm(DME)** are observed at δ = 0.30, 4.14 and 11.49 ppm, the Tp-borohydride at δ = −1.20 ppm, and the DME ligand protons at δ = 3.29 and 3.42 ppm, in the expected 6 : 6 : 6 : 2 : 6 : 4 ratio. The proton and carbon resonances of the Tp ligands and DME of **1-Sm(DME)** were assigned using DEPT-135 ^{13}C{^{1}H} and ^{1}H-^{13}C HSQC NMR experiments (see ESI Fig. S10 and Fig. S11,† respectively). The ^{11}B NMR spectrum of **1-Sm(DME)** exhibits a resonance at δ = −25.36 ppm, corresponding to the Tp ligands, consistent with [Sm(Tp^R)$_2$].[29,30e] The ATR-IR spectra of **1-Sm** and **1-Sm(DME)**, both exhibit weak absorptions between 2350–2450 cm^{-1} assigned to the characteristic borohydride stretching frequencies (υ_{BH}) for the Tp ligands in Ln(II) [Ln(Tp^R)$_2$][29,30f] and [Ln(Tp)$_2$] complexes.[31] Additionally, weak absorptions are observed between 2820–2930 cm^{-1}, which are assigned to the aliphatic sp^3-carbon hydrogen bond stretching frequencies ($\upsilon_{sp^3\text{-}CH}$) of the DME ligand in **1-Sm(DME)**, consistent with literature.[39]

Crystallography of [Sm(Tp)$_2$(LB)$_x$] (LB = THF, *x* = 2; DME, *x* = 1) 1-Sm(LB)

Lath-shaped red single-crystals of **1-Sm(THF)** suitable for X-ray diffraction were grown from a saturated THF solution at −35 °C overnight and shard-shaped red single-crystals of **1-Sm(DME)** suitable for X-ray diffraction were grown from a saturated toluene solution with a hexane antisolvent at −35 °C over three weeks. The structures of **1-Sm(LB)** are monomeric, containing an 8-coordinate Sm(II) ion bound to two κ^3-coordinated Tp ligands and two oxygen atoms for two THF adducts (Fig. 2(a)) or one DME adduct (Fig. 2(b)), arranged around the Sm(II) ion in a distorted square antiprismatic geometry. Important structural metrics are tabulated in the ESI in section B,† with bond metrics and relevant structural data

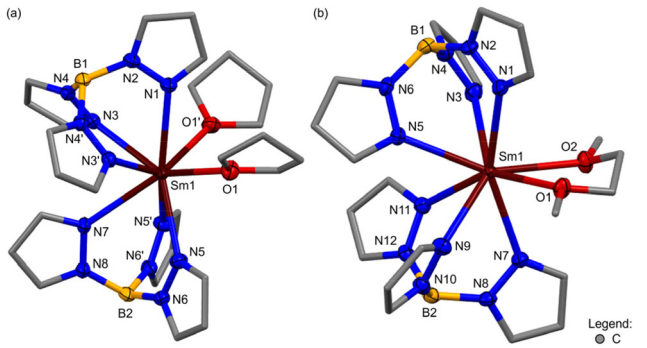

Fig. 2 Molecular structures of $[Sm(Tp)_2(LB)_x]$ **1-Sm(LB)** LB = THF (a), DME (b). Hydrogen atoms and lattice solvent molecules omitted for clarity and carbon atoms of Tp pyrazolyl, THF, and DME displayed in wire-frame. Displacement ellipsoids drawn at 50% probability level. Selected bond distances: (a) Sm–N(Tp) 2.662(6)–2.744(7) Å, Sm–O(THF) 2.692(4) Å, (b) Sm–N(Tp) 2.6805(16)–2.7180(16) Å, Sm–O(DME) 2.6696(14), 2.7044(14) Å.

comparisons in Table 1 and crystallographic information in Table 2.† The Sm–N(Tp) bond distances in **1-Sm(LB)** (LB = THF, 2.662(6)–2.744(7) Å; DME, 2.6805(16)–2.7180(16) Å) are indistinguishable to those in the Eu(II) complex $[Eu(Tp)_2(THF)_2]$ and longer than those in the Yb(II) complexes $[Yb(Tp)_2(LB)]$ (LB = THF, DME) consistent with the size of the different Ln(II) ionic radii Sm(II) ~ Eu(II) ≫ Yb(II).[31,38] The Sm–N(κ^3-Tp) bond distances in **1-Sm(LB)** are consistent with adduct-free $[Sm(Tp^R)_2]$ (see ESI Table 1†).[23,29,30e] Since a range of Ln–N(κ^3-Tp) bond distances is normally observed in literature $[Ln(Tp^R)_2]$ complexes (ESI Table 1†), therefore small structural differences *e.g.* neighbouring Ln(II) ionic radii or substitution of the Tp ligand (Tp^R) do not result in statistically significant Ln–N(κ^3-Tp) distances. The increase in ionic radius upon reduction of Sm(III) to Sm(II) is reflected by the longer Sm–N(Tp) bond distances in **1-Sm(LB)** when compared to the THF-adduct of the Sm(III) precursor $[Sm(Tp)_2(OTf)(THF)]$ (2.512(2)–2.583(2) Å).[32c]

Reactivity of 1-Sm(DME) with molecular pnictogens

Owing to the diverse reactivity exhibited by $[Sm(Tp^R)_2]$,[18–28] the scope of **1-Sm(DME)** in small-molecule activation was investigated in collaboration with the Roesky group. Since the reactivity of Ln(II) $[Ln(Tp^R)_2]$ with pnictogens has not been reported to date, the reactivity of **1-Sm(DME)** with white phosphorus (P_4) was tested, targeting motifs such as $[\{(Cp^*)_2Sm\}_4(\mu^4\text{-}\eta^2\text{:}\eta^2\text{:}\eta^2\text{:}\eta^2\text{-}P_8)]$.[13a,40] Reactions of **1-Sm(DME)** with freshly sublimated P_4 or P_4 vapour, resulted in formation of insoluble Sm(III) products, where $[Sm(Tp)_3]$[41] was crystallised on several occasions as the major product, irrespective of reaction conditions and solvents. Reactions of $[Yb(Tp)_2]$[31] with white P_4, led to the formation of $[Yb(Tp)_3]$[36a] and recovery of unreacted $[Yb(Tp)_2]$, consistent with the lower reducing strength of Yb(II) *vs.* Sm(II).[34] Reactivity of **1-Sm(DME)** with heavier pnictogens like elemental nanoparticles of arsenic (As^0_{nano}),[42] were also unsuccessful.

Reactivity of 1-Sm(DME) with carbon dioxide (CO_2) in the synthesis of $[\{Sm(Tp)_2\}_2(\mu\text{-}\eta^2\text{:}\eta^2\text{-}O_2CCO_2)]$ 2-Sm

Activation and functionalisation of CO_2 by Sm(II) in various ligand environments have been reported in literature to yield oxalate-bridged Sm(III) dimers (Fig. 1(a)).[7a–e] The synthesis of the oxalate-bridged dimeric Ln(III) complexes $[\{Ln(Tp)_2\}_2(\mu\text{-}\eta^2\text{:}\eta^2\text{-}O_2CCO_2)]$ (Ln = Y, Sm, Dy, Yb, Lu) were previously reported by salt metathesis between Ln(III) chlorides $[LnCl_3.(H_2O)_n]$, K(Tp), and $Na_2(C_2O_4)$ in a 2 : 4 : 1 ratio in water.[43] Since the reactivity of Ln(II) $[Ln(Tp^R)_2]$ with CO_2 has not been reported to date, the reaction of **1-Sm(DME)** with CO_2 was studied in d_8-THF to yield the Sm(III) complex $[\{Sm(Tp)_2\}_2(\mu\text{-}\eta^2\text{:}\eta^2\text{-}O_2CCO_2)]$ **2-Sm** (92%, Scheme 2). Complex **2-Sm** has poor solubilities in all solvents. Elemental analysis of **2-Sm** is consistent with the $[\{Sm(Tp)_2\}_2(\mu\text{-}\eta^2\text{:}\eta^2\text{-}O_2CCO_2)]$ formulation.

Spectroscopy of $[\{Sm(Tp)_2\}_2(\mu\text{-}\eta^2\text{:}\eta^2\text{-}O_2CCO_2)]$ 2-Sm

Due to the insolubility of **2-Sm** post-work-up, the NMR data discussed here are from the NMR-scale reaction of **1-Sm(DME)** with CO_2 in d_8-THF (see ESI section A2.1†). In the ^1H NMR spectrum of **2-Sm** in d_8-THF, the Tp-pyrazolyl protons in **2-Sm** are observed at δ = 4.87, 6.04 and 8.84 ppm, consistent with NMR of this complex reported elsewhere.[43] The proton and carbon resonances of the pyrazolyl rings of the Tp ligands of **2-Sm** were assigned as far as possible, by using $^{13}C\{^1H\}$ and ^1H–^{13}C HSQC NMR experiments (see ESI Fig. S45 and Fig. S46,† respectively). In the $^{13}C\{^1H\}$ NMR spectrum of **2-Sm**, the resonance corresponding to the oxalate ligand carbon could not be identified. This observation is similar to the $^{13}C\{^1H\}$ NMR spectra of $[\{Sm(Cp^R)_2\}_2(\mu\text{-}\eta^2\text{:}\eta^2\text{-}O_2CCO_2)]$,[7a,b] where the oxalate ligand carbon atoms were not observed unless reactions were performed with $^{13}CO_2$.[7a] The ^{11}B NMR spectrum of **2-Sm** exhibits a resonance at δ = 2.91 ppm, corresponding to the Tp ligands, consistent with other $[Sm(Tp)_2]^+$ examples.[32c] In the ATR-IR spectrum of **2-Sm**, besides weak absorptions between 2350–2450 cm^{-1} assigned to the characteristic borohydride stretching frequencies (υ_{BH}) for the Tp ligands, a weak absorption is also observed at 1649 cm^{-1}, which is assigned to

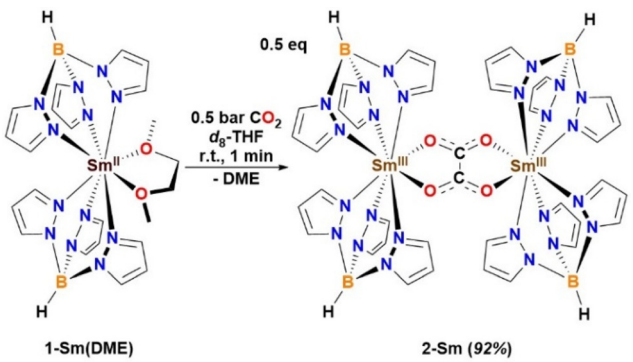

Scheme 2 Reaction of **1-Sm(DME)** with CO_2 to yield oxalate-bridged dimeric Sm(III) complex $[\{Sm(Tp)_2\}_2(\mu\text{-}\eta^2\text{:}\eta^2\text{-}O_2CCO_2)]$ **2-Sm**.

the carbonyl stretching frequencies ($\upsilon_{C=O}$) of the oxalate ligand in **2-Sm**, analogous to reported [{Ln(Tp)$_2$}$_2$(μ-η^2:η^2-O$_2$CCO$_2$)] (Ln = Y, La, Ce, Nd, Sm, Dy, Yb, Lu) ($\upsilon_{C=O}$ = 1620–1660 cm^{-1}).[43]

Crystallography of [{Sm(Tp)$_2$}$_2$(μ-η^2:η^2-O$_2$CCO$_2$)] 2-Sm

The solid-state structure of **2-Sm** was not previously reported.[43] Block-shaped colourless single-crystals of **2-Sm** suitable for X-ray diffraction were grown from a saturated THF solution with a hexane antisolvent at −35 °C over four months. The structure of **2-Sm** (Fig. 3) is dimeric, containing two 8-coordinate Sm(III) ions where each Sm(III) ion is bound to two κ^3-coordinated Tp ligands and two oxygens of the μ-η^2:η^2-O$_2$CCO$_2^{2-}$ oxalate ligand bridging the two Sm(III) ions, in a distorted square antiprismatic geometry. The Sm–N(κ^3-Tp) bond distances of 2.480(6)–2.592(7) Å in **2-Sm** are consistent with [Sm(Tp)$_2$]$^+$.[32c] The Sm–O(C$_2$O$_4$) bond distances of 2.423(6) and 2.425(5) Å in **2-Sm** are consistent with the literature of oxalate-bridged dimeric Sm(III) complexes (see ESI Table 1†).[7b,d] The Sm–N(κ^3-Tp) and Sm–O(C$_2$O$_4$) bond distances in **2-Sm** are longer than those in [{Dy(Tp)$_2$}$_2$(μ-η^2:η^2-O$_2$CCO$_2$)] (see ESI Table 1†) and consistent with differences in size of the different Ln(III) ionic radii Sm(III) > Dy(III).[38]

Reactivity of [Ln(Tp)$_2$(N″)] (Ln = Y, Sm; N″ = N(SiMe$_3$)$_2$ with CO$_2$) in the synthesis of [Ln(Tp)$_2$(OSiMe$_3$)] 3-Ln

The heteroleptic Ln(III) amide complexes [Ln(Tp)$_2$(N″)] (Ln = Y, Yb, Dy) are reactive towards protonolysis with alcohols[32a] and primary amines.[32b] To aid investigation of CO$_2$ activation by the paramagnetic [Sm(Tp)$_2$(N″)], the analogous diamagnetic reaction with Ln = Y was also studied. Reactions of d_6-benzene solutions of [Ln(Tp)$_2$(N″)] (Ln = Y,[32a] Sm)[32c] with CO$_2$ led to the complete consumption of [Ln(Tp)$_2$(N″)]. The reaction proceeds likely by insertion of CO$_2$ to form the carbamate intermediate [Ln(Tp)$_2$(κ^2-O,OCN″)] (see Fig. 1(b)(i)),[2a,10b] which is not observed, but the subsequent intermediate complex [Ln(Tp)$_2$(κ^2-O,O(SiMe$_3$)C=NSiMe$_3$)] resulting from an intramolecular silyl-migration (see Fig. 1(b)(ii)), was observed on the NMR-scale (see ESI section A2.2† for Ln = Y and section A2.3 for Ln = Sm). Upon work up of the reaction mixtures by removing d_6-benzene, excess CO$_2$, and O=C=NSiMe$_3$ *in vacuo*, and washing the crude with hexane, the monomeric Ln(III) silyloxides [Ln(Tp)$_2$(OSiMe$_3$)] **3-Ln** (Ln = Y, 59%, Sm 53%; Scheme 3) were isolated. Complexes **3-Ln** have excellent solubilities in toluene and moderate solubilities in hexane.

The [Ln(Tp)$_2$(N″)] complexes are air/moisture-sensitive and adventitious moisture-mediated decomposition of [Y(Tp)$_2$(N″)] yields the hydroxide-bridged dimer [{Y(Tp)$_2$(μ-OH)}$_2$].[32a] On one occasion during exploration of the reactivity of [Sm(Tp)$_2$(N″)] with small-molecules, similar adventitious moisture-mediated decomposition of [Sm(Tp)$_2$(N″)] yielded a hydroxide-bridged cluster [Sm$_5$(Tp)$_6$(μ$_2$-OH)$_6$(μ$_3$-OH)$_2$(μ$_4$-OH)] **4-Sm** (see ESI section A1.6† for NMR data for **4-Sm** and Fig. S69† for the connectivity-only molecular structure of **4-Sm**). The formation of a hydroxide-bridged {Sm$_5$} cluster instead of a hydroxide-bridged {Ln$_2$} dimer as seen for Y(III) is consistent with the larger size of the Sm(III) ion when compared to the Y(III) ion.[38]

Spectroscopy of [Ln(Tp)$_2$(OSiMe$_3$)] 3-Ln (Ln = Y, Sm)

In the ^{1}H NMR spectrum of **3-Y** in d_6-benzene, the Tp-pyrazolyl protons in **3-Y** are observed at δ = 5.81, 7.26 and 7.49 ppm, the Tp-borohydride at δ = 4.82 ppm, and the trimethylsilyl protons at δ = −0.06 ppm, in the expected 6 : 6 : 6 : 2 : 9 ratio. In the ^{1}H NMR spectrum of **3-Sm** in d_6-benzene, the Tp-pyrazolyl protons in **3-Sm** are observed at δ = 2.61, 5.64 and 8.96 ppm, the Tp-borohydride at δ = 8.22 ppm, and the trimethylsilyl protons at δ = 2.56 ppm, in the expected 6 : 6 : 6 : 2 : 9 ratio. The OSiMe$_3$ ligand resonance in **3-Y** is comparable to that observed in [Y{2,2′-bis-((ᵗBuMe$_2$Si)N)-6,6′-Me$_2$-biphenyl}(OSiMe$_3$)(THF)$_2$] (δ = 0.26 ppm).[44] The proton and carbon resonances of the Tp ligands and the OSiMe$_3$ ligand of **3-Ln** were assigned by using ^{13}C{^{1}H} and ^{1}H-^{13}C HSQC NMR experiments. The ^{11}B NMR spectra of **3-Ln** exhibit a resonance (δ = −2.93 ppm **3-Y**, δ = 5.43 ppm **3-Sm**), corresponding to the Tp ligands, similar to

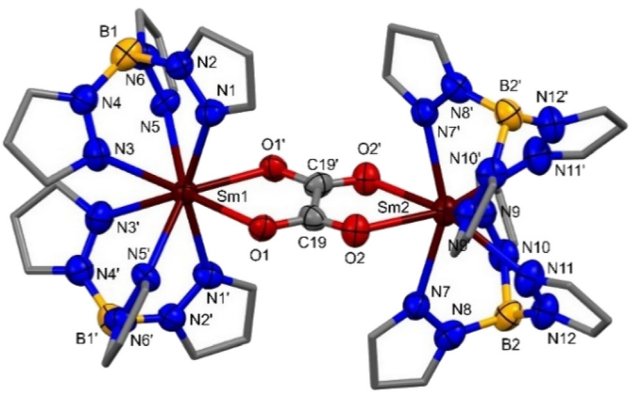

Fig. 3 Molecular structure of [{Sm(Tp)$_2$}$_2$(μ-η^2:η^2-O$_2$CCO$_2$)] **2-Sm**. Hydrogen atoms and lattice solvent molecules omitted for clarity and carbon atoms of Tp pyrazolyl displayed in wireframe. Displacement ellipsoids drawn at 50% probability level. Selected bond distances: Sm–N(Tp) 2.480(6)–2.592(7) Å, Sm–O(C$_2$O$_4$) 2.423(6), 2.425(5) Å.

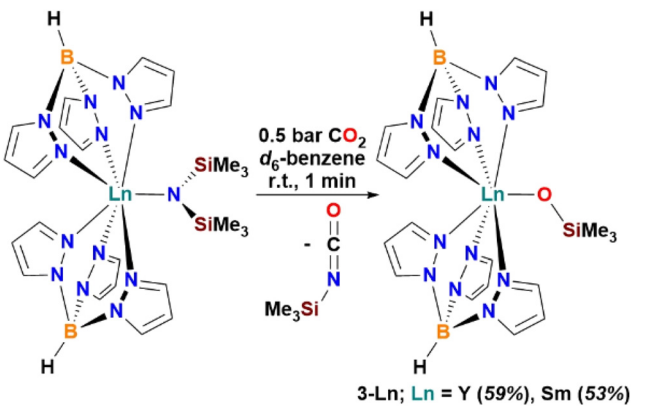

Scheme 3 CO$_2$ activation by Ln(III) complexes [Ln(Tp)$_2$(N″)] (Ln = Y, Sm; N″ = N(SiMe$_3$)$_2$) to yield monomeric Ln(III) silyloxides [Ln(Tp)$_2$(OSiMe$_3$)] **3-Ln**.

the chemical shifts observed in the amide complexes $[Ln(Tp)_2(N'')]$ (Ln = Y, δ = −2.96 ppm;[32a] Sm, δ = 6.25 ppm).[32c] In the ATR-IR spectrum of **3-Ln**, besides weak absorptions between 2350–2470 cm^{-1} assigned to the characteristic borohydride stretching frequencies (υ_{BH}) for the Tp ligands, weak absorptions were also observed between 2890–2960 cm^{-1}, which are assigned to the aliphatic sp^3-carbon hydrogen bond stretching frequencies ($\upsilon_{sp^3\text{-}CH}$) of the $OSiMe_3$ ligand.[16,44]

Crystallography of $[Ln(Tp)_2(OSiMe_3)]$ 3-Ln (Ln = Y, Sm)

Rod-shaped colourless single-crystals of **3-Y** suitable for X-ray diffraction were grown from a saturated d_6-benzene solution with a hexane antisolvent at −35 °C overnight, and tablet-shaped colourless single-crystals of **3-Sm** suitable for X-ray diffraction were grown from a saturated hexane solution at −35 °C over three months. The structures of **3-Ln** are monomeric, containing a 7-coordinate Ln(III) ion bound to two κ^3-coordinated Tp ligands and a monodentate $OSiMe_3$ anion, arranged around the Ln(III) ion in a pentagonal bipyramidal geometry (Fig. 4). The $[Ln(Tp)_2(\kappa^2\text{-}O,O(SiMe_3)C{=}NSiMe_3)]$ intermediate in the formation of **3-Ln** could not be isolated by crystallisation of the crude reaction mixtures, since **3-Ln** was crystallised from all attempts. The Ln–N(Tp) bond distances (**3-Sm**: 2.538(3)–2.589(3) Å, **3-Y**: 2.451(6)–2.567(8) Å) and Ln–O ($OSiMe_3$) bond distances (**3-Sm:** 2.155(2) Å, **3-Y**: 2.094(6) Å), are consistent with differences in size of the different Ln(III) ionic radii Sm(III) > Y(III) and the fact that a range of Ln–N(κ^3-Tp) bond distances is normally observed in the literature $[Ln(Tp)_2]^+$ complexes.[38] The Ln–N(κ^3-Tp) bond distances in **3-Ln** are consistent with $[Ln(Tp)_2(X)]$.[32] The Ln–O($OSiMe_3$) bond distances in **3-Ln** are consistent with heteroleptic monomeric Ln(III) silyloxides containing Ln–O($OSiMe_3$) (Ln = Y,[44,45] Sm)[46] bonds and homoleptic monomeric Ln(III) silyloxides $[Ln(OSiR_3)_3(LB)_x]$ (Ln = Y, R = O^{t}Bu,[47] Ph;[48] Sm, R = $SiMe_3$,[49] Ph)[50] (see ESI Table 1† for detailed data comparisons). The Sm–N(Tp) bond distances in **3-Sm** are shorter than those in **1-Sm(LB)**, consistent with the smaller ionic radius of Sm(III) *vs.* Sm(II).[38]

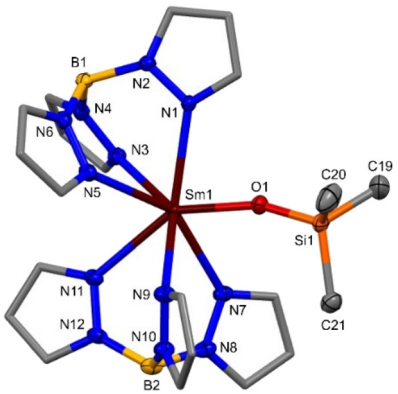

Fig. 4 Molecular structure of **3-Sm** (see ESI Fig. S67† for the molecular structure of **3-Y**). Hydrogen atoms omitted for clarity and pyrazolyl carbon atoms of Tp displayed in wireframe. Displacement ellipsoids drawn at 50% probability level. Selected bond distances in **3-Sm**: Sm–N(Tp) 2.538(3)–2.589(3) Å, Sm–O($OSiMe_3$) 2.155(2) Å; Selected bond distances in **3-Y**: Y–N(Tp) 2.451(6)–2.567(8) Å, Y–O($OSiMe_3$) 2.094(6) Å.

Conclusions

The reduction of heteroleptic Ln(III) triflate complexes $[Ln(Tp)_2(OTf)]$ (Tp = hydrotris(1-pyrazolyl)borate; OTf = triflate) was successfully extended to Sm(II). The reduction of $[Sm(Tp)_2(OTf)]$ with KC_8 in THF yielded the insoluble Sm(II) $[\{Sm(Tp)_2\}_n]$ **1-Sm** multi-metallic coordination polymer, which was successfully isolated as the monomeric 1,2-dimethoxyethane (DME) adduct complex $[Sm(Tp)_2(DME)]$ **1-Sm(DME).** The reactivity of **1-Sm(DME)** was investigated with various small molecules such as pnictogens and CO_2. The reactions of **1-Sm(DME)** with molecular pnictogens (white P_4, As^0_{nano}) yielded intractable Sm(III) products and $[Sm(Tp)_3]$. The reaction of **1-Sm(DME)** with CO_2 yielded the oxalate-bridged dimeric Sm(III) homobimetallic complex $[\{Sm(Tp)_2\}_2(\mu\text{-}\eta^2\text{:}\eta^2\text{-}O_2CCO_2)]$ **2-Sm.** Furthermore, CO_2 activation by lanthanide silylamide complexes in the bis-Tp ligand environment was investigated. Reactions of the heteroleptic Ln(III) amides $[Ln(Tp)_2(N'')]$ (Ln = Y, Sm; N'' = $N(SiMe_3)_2$) with CO_2, was proposed to proceed *via* formation a carbamate intermediate $[Ln(Tp)_2(\kappa^2\text{-}O,OCN'')]$, which was not observed, but the subsequent intermediate $[Ln(Tp)_2(\kappa^2\text{-}O,O(SiMe_3)C{=}NSiMe_3)]$ in this pathway, resulting from an intramolecular silyl-migration was observed on the NMR-scale. Upon workup of the reaction mixtures and removal of the CO_2-functionalised product $O{=}C{=}NSiMe_3$, the monomeric Ln(III) silyloxides $[Ln(Tp)_2(OSiMe_3)]$ **3-Ln** were isolated. The bis-Tp ligand environment on the Ln(III) ion enabled isolation of **3-Ln** as discrete molecular silyloxides, which are the first crystallographically characterised examples of Ln(III)–$OSiMe_3$ bonds accessed *via* CO_2 activation and functionalisation.

Experimental

General experimental considerations

All air-sensitive manipulations were carried out in an MBraun glovebox (inert atmosphere of N_2, O_2 < 0.1 ppm, H_2O < 1.5 ppm) or by using standard Schlenk techniques under N_2. All glassware was dried at 130 °C overnight, in a Binder ED53 Drying Oven/Hot Air Steriliser, prior to use. An Innovative Technology Inc. Pure Solv 400-5-MD solvent purification system (activated alumina columns) was used to obtain anhydrous toluene and tetrahydrofuran (THF). Anhydrous hexane (95%) and 1,2-dimethoxyethane (DME, 99.5%) were purchased from Merck. Anhydrous solvents were degassed, sparged with N_2, and stored in ampoules over activated 3.0 Å molecular sieves (25–35% weight by volume) under N_2. Absence of water/levels of residual water in bulk solvents were confirmed by using a sodium benzophenone ketyl solution in THF after 24–48 hours. Deuterated benzene (d_6-benzene) and deuterated

THF (d_8-THF) were purchased from Merck and dried by directly transferring from sealed glass ampoules onto activated 3.0 Å molecular sieves and stored in ampoules in a N_2 atmosphere glovebox. Deuterated toluene (d_8-toluene) was purchased from Merck and degassed by three freeze–pump–thaw degassing cycles and dried by storing in ampoules over activated 3.0 Å molecular sieves in a N_2 atmosphere glovebox. Deuterated acetonitrile (d_3-MeCN) was purchased from Merck and dried by refluxing over CaH_2, degassed by three freeze–pump–thaw degassing cycles, filtered across a frit coated with Celite® into a Büchner flask, to exclude excess CaH_2 and stored in ampoules over activated 3.0 Å molecular sieves in a N_2 atmosphere glovebox. Absence of water in deuterated solvents was confirmed by ^{1}H NMR after 48 hours. Carbon dioxide (CO_2, 99.98%, vapour withdrawal) was purchased from BOC. Potassium hydrotris(1-pyrazolyl)borate K(Tp), K(N″) (N″ = $N(SiMe_3)_2$), $Ln(OTf)_3$ (OTf = CF_3SO_3; Ln = Y, Sm, Dy), $[Ln(Tp)_2(OTf)]$ (Ln = Y, Sm, Dy), $[Ln(Tp)_2(N'')]$ (Ln = Y, Sm), were synthesised according to published procedures.[32]

Physical methods

NMR data were recorded on an AVIII 400 MHz spectrometer operating at frequencies 400.1 MHz (^{1}H), 100.6 MHz (^{13}C{^{1}H}), 128.4 MHz (^{11}B and ^{11}B{^{1}H}). The NMR data were referenced internally to the appropriate residual proteo-solvent and reported relative to tetramethylsilane (δ = 0 ppm) for ^{1}H and ^{13}C{^{1}H} NMR. ^{11}B and ^{11}B{^{1}H} NMR data were reported relative to 15% $BF_3{\cdot}OEt_2$ in $CDCl_3$ (δ = 0 ppm). All spectra were recorded at a constant temperature of 25 °C (298 K). Coupling constants (J) are reported in hertz (Hz). Standard abbreviations for multiplicity were used as follows: m = multiplet, t = triplet, d = doublet, s = singlet. For broad intensities, abbreviated as br, the full width at half-maximum intensity (FWHM) is provided in Hz. ATR-IR spectra were collected in air at ambient temperature using ThermoFisher Scientific Nicolet Summit LITE FTIR Spectrometer (containing a $LiTaO_3$ detector) equipped with Everest ATR. Abbreviations for the intensity of stretching frequencies were used as follows: s = strong, m = medium, w = weak. Single-crystal X-ray diffraction data for **1-Sm(THF)**, **1-Sm(DME)**, **Y-pz**, **3-Y**, and **3-Sm** were collected at 150 K using Mo-K_α radiation (λ = 0.71073 Å) on a Bruker D8 VENTURE diffractometer equipped with a Photon II CPAD detector, with Oxford Cryosystems n-Helix device mounted on an IμS 3.0 (dual Cu and Mo) microfocus sealed tube generator. Single-crystal X-ray diffraction data for **2-Sm** (on beamline I19 at the Diamond Light Source) and **4-Sm** were collected by the EPSRC UK National Crystallography Service (University of Southampton). Deposition numbers 2347954–2347960† contain the supplementary crystallographic data for this paper. Elemental analyses were performed by Orla McCullough at the London Metropolitan University, using a Flash 2000 Organic Elemental Analyzer, Thermo Scientific analyser. The samples for the measurements were prepared using V_2O_5 (to ensure complete combustion of all complexes) in tin capsules inside an inert argon glovebox atmosphere.

Synthesis of Sm(II) $[\{Sm(Tp)_2\}_n]$ 1-Sm and $[Sm(Tp)_2(LB)_x]$ (LB = THF, x = 2; DME, x = 1) 1-Sm(LB)

Synthesis of $[\{Sm(Tp)_2\}_n]$ 1-Sm *via* $[Sm(Tp)_2(THF)_2]$ 1-Sm (THF). In the glovebox, a 20 mL scintillation vial was charged with a stirrer bar, and then the white powder $[Sm(Tp)_2(OTf)]$ (92.1 mg, 0.127 mmol, 1.0 eq.) was dissolved in THF (3 mL) and stirred. To this colourless solution, the bronze powder KC_8 (34.4 mg, 0.255 mmol, 2.0 eq.) was added by spatula in small portions over two minutes, with stirring at ambient temperature. The resultant dark-red suspension was stirred at ambient temperature for 0.5 h, after which the colour of the suspension darkened to a deep red-brown colour and was filtered across a frit into a Büchner flask, to exclude excess KC_8 and graphite. Further product was extracted from the black solids on the frit with THF (2 mL), the deep orange filtrates were combined, and THF (5 mL) was removed *in vacuo*. The resultant red-brown solids containing $[Sm(Tp)_2(THF)_2]$ **1-Sm (THF)** were dried *in vacuo* (10^{-2} mbar, 1 h). Toluene (8 mL) was added, and the resultant dark orange-brown suspension was vigorously shaken and subsequently filtered across a frit into a Büchner flask, to exclude K(OTf). Further product was extracted from the solids on the frit with toluene (1 mL), the dark orange-brown filtrates were combined, and toluene (9 mL) was removed *in vacuo*. The resultant dark-brown solid was scraped with a spatula and the powder was dried *in vacuo* (10^{-2} mbar, 2 h) yielding adduct-free $[\{Sm(Tp)_2\}_n]$ **1-Sm** (66.4 mg, 0.116 mmol, 91%). The multi-metallic coordination polymer **1-Sm** has extremely poor solubility in all solvents. Anal. Calcd for $(C_{18}H_{20}B_2N_{12}Sm)_n$: C, 37.51%; H, 3.50%; N, 29.16%. Found: C, 38.39%; H, 3.66%; N, 25.78%. Note: The discrepancy in the percentage of nitrogen in the elemental analyses of $[Ln(Tp)_2(X)]$ and $[Ln(Tp)_2]$ complexes have been routinely observed to be off by *ca.* 2.5–3.0%.[31,32] IR (ATR): 3143 (w, $\upsilon_{sp^2\text{-}CH}$), 3116 (w, $\upsilon_{sp^2\text{-}CH}$), 2445 (w, υ_{BH}), 2406 (w, υ_{BH}), 2372 (w, υ_{BH}), 1726 (w), 1614 (w), 1505 (m, $\upsilon_{C=C}$), 1402 (s), 1384 (s), 1293 (s), 1209 (s), 1118 (s), 1045 (s), 973 (s), 925 (w), 876 (w), 803 (w), 752 (s), 722 (s), 668 (s), 620 (s) cm^{-1}. The multinuclear NMR data below for **1-Sm(THF)** was obtained by extracting product into d_8-toluene from the dried filtrate in THF (after synthesis) and the data were collected within 12 hours. ^{1}H NMR (d_8-toluene): δ −3.64 (2H, very br m, FWHM = 289.4 Hz, Tp-B**H**) −1.56 (6H, s, FWHM = 25.0 Hz, Tp-C**H**), 0.18 (8H, s, FWHM = 19.9 Hz, THF-C**H$_2$**), 2.27 (8H, s, FWHM = 27.2 Hz, THF-C**H$_2$**), 4.02 (6H, s, FWHM = 26.3 Hz, Tp-C**H**), 15.10 (6H, very br s, FWHM = 106.4 Hz, Tp-C**H**) ppm; ^{13}C{^{1}H} NMR (d_8-toluene): δ 25.3 (s, THF-**C**), 74.2 (s, Tp-**C**), 85.0 (very br s, THF-**C**), 112.7 (s, Tp-**C**), 204.7 (br s, Tp-**C**) ppm; ^{11}B NMR (d_8-toluene): δ −32.00 (d, $^1J_{B-H}$ = 82.4 Hz, Tp-**B**) ppm; ^{11}B{^{1}H} NMR (d_8-toluene): δ −32.00 (s, Tp-**B**) ppm. Desolvation of THF-adducts from **1-Sm(THF)** is observed in solution in 48 hours in d_8-toluene. When heated up to 65 °C in d_8-toluene, **1-Sm(THF)** desolvates completely in an hour, liberating free THF, **1-Sm**, and $[Sm(Tp)_3]$. Lath-shaped red single-crystals of $[Sm(Tp)_2(THF)_2{\cdot}(THF)]$ **1-Sm(THF)** suitable for X-ray diffraction were grown from a saturated THF solution at −35 °C overnight.

Synthesis of [Sm(Tp)$_2$(DME)] 1-Sm(DME) *via* 1-Sm(THF). With the reagents and measures [Sm(Tp)$_2$(OTf)] (95.6 mg, 0.132 mmol, 1.0 eq.) and KC_8 (35.5 mg, 0.263 mmol, 2.0 eq.), **1-Sm(THF)** was generated *in situ* analogously as above and extracted into toluene with filtration to exclude K(OTf). Toluene (7.5 mL) was removed *in vacuo* from the combined dark brown filtrate, to yield a dark brown solid. DME (0.5 mL) was added to the dark brown solid to immediately result in the formation of a dark violet-brown solution, which was evaporated to dryness yielding dark violet-brown solids. The solids were scraped with a spatula and the resultant violet-brown powder was dried *in vacuo* (10^{-2} mbar, 2 h) yielding [Sm(Tp)$_2$(DME)] **1-Sm(DME)** (78.5 mg, 0.118 mmol, 89%). Complex **1-Sm(DME)** is very air/moisture sensitive. In the solid-state it is stable under the glovebox conditions and stable for up to 3 months in dry coordinating solvents such as THF. Complex **1-Sm(DME)** is also stable in non-coordinating solvents such as benzene and toluene at ambient temperature, where slow desolvation of DME from **1-Sm(DME)** is observed and complete desolvation, with some decomposition, is observed within 1–2 weeks in d_6-benzene. Complex **1-Sm(DME)** reacts with d_3-MeCN, leading to complicated reaction mixtures containing multiple Sm(III) species. Shard-shaped red single-crystals of [Sm(Tp)$_2$(DME)·(toluene)] **1-Sm(DME)** suitable for X-ray diffraction were grown from a saturated toluene solution with a hexane antisolvent at −35 °C over three weeks. ^{1}H NMR (d_8-THF): δ −1.20 (2H, very br m, FWHM = 309.9 Hz, Tp-B**H**), 0.30 (6H, br s, FWHM = 36.8 Hz, Tp-C**H**), 3.29 (6H, s, DME-C**H$_3$**), 3.42 (4H, s, DME-C**H$_2$**), 4.14 (6H, s, FWHM = 17.2 Hz, Tp-C**H**), 11.49 (6H, br s, FWHM = 35.3 Hz, Tp-C**H**) ppm; ^{13}C{^{1}H} NMR (d_8-THF): δ 59.1 (s, DME-**C**H$_3$), 72.9 (s, DME-**C**H$_2$), 75.8 (br s, Tp-**C**), 115.4 (br s, Tp-**C**), 193.1 (br s, Tp-**C**) ppm; ^{11}B NMR (d_8-THF): δ −25.36 (d, $^1J_{B-H}$ = 74.7 Hz, Tp-**B**) ppm; ^{11}B{^{1}H} NMR (d_8-THF): δ −25.42 (s, Tp-**B**) ppm. Anal. Calcd for $C_{22}H_{30}B_2N_{12}O_2Sm$: C, 39.64%; H, 4.54%; N, 25.22%. Found: C, 39.01%; H, 4.26%; N, 23.94%. IR (ATR): 3147 (w, $\upsilon_{sp^2\text{-}CH}$), 3117 (w, $\upsilon_{sp^2\text{-}CH}$), 2928 (w, $\upsilon_{sp^3\text{-}CH}$), 2888 (w, $\upsilon_{sp^3\text{-}CH}$), 2825 (w, $\upsilon_{sp^3\text{-}CH}$), 2446 (w, υ_{BH}), 2411 (w, υ_{BH}), 2375 (w, υ_{BH}), 1728 (w), 1616 (w), 1503 (m, $\upsilon_{C=C}$), 1402 (s), 1386 (s), 1296 (s), 1211 (s), 1118 (s), 1040 (s), 973 (s), 923 (w), 887 (w), 854 (w), 805 (w), 752 (s), 720 (s), 664 (s), 620 (s) cm^{-1}.

Reaction of [Dy(Tp)$_2$(OTf)] with KC_8 in toluene resulting in the observation of [Dy(Tp)$_3$]

In the glovebox, a 20 mL scintillation vial was charged with a stirrer bar, and then the white powder [Dy(Tp)$_2$(OTf)] (31.6 mg, 0.043 mmol, 1.0 eq.) was suspended in toluene (3 mL) and stirred. To this white suspension, the bronze powder KC_8 (10.9 mg, 0.081 mmol, 1.9 eq.) was added by spatula in small portions over two minutes, with stirring at ambient temperature. The resultant dark-brown suspension was stirred at ambient temperature for 22.5 h, after which the resultant black-brown suspension was filtered across a frit into a Büchner flask, to exclude excess KC_8, graphite, and K(OTf). Toluene (3 mL) was removed *in vacuo* to yield a dark orange-brown solid, which was dried *in vacuo* (10^{-2} mbar, 4.5 h). Subsequently, d_6-benzene (0.5 mL) was added, and the resultant orange solution was analysed *via* multinuclear NMR to show the NMR resonances consistent with [Dy(Tp)$_3$][36b] as a major product amongst other unidentified Dy(III) products.

Reaction of [Y(Tp)$_2$(OTf)] with KC_8 in THF resulting in isolation of [Y(Tp)$_2$(κ^2-pz)] Y-pz (pz = pyrazolyl)

In the glovebox, a 20 mL scintillation vial was charged with a stirrer bar, and then the white powder [Y(Tp)$_2$(OTf)·(toluene)$_{0.07}$] (42.2 mg, 0.063 mmol, 1.0 eq.) was dissolved in THF (3.5 mL) and stirred. To this colourless solution, the bronze powder KC_8 (20.0 mg, 0.148 mmol, 2.4 eq.) was added by spatula in small portions over two minutes, with stirring at ambient temperature. The resultant dark-brown suspension was stirred at ambient temperature for 20 h, after which the suspension was filtered across a frit into a Büchner flask, to exclude excess KC_8 and graphite. THF (3.5 mL) was removed *in vacuo* to yield a yellow-brown oil, which was dried *in vacuo* (10^{-2} mbar, 1.5 h). The yellow-brown oil was washed with hexane (3 × 1 mL) and the washings filtered through a pipette containing a Kimwipe. The pale-yellow filtrate was cooled down to −35 °C and the product [Y(Tp)$_2$(κ^2-pz)] **Y-pz** crystallised overnight as colourless plates, including crystals of [Y(Tp)$_3$] (see ESI Fig. S17(b)† for overlay of ^{1}H NMR data for **Y-pz** and [Y(Tp)$_3$][32b]). ^{1}H NMR (d_6-benzene): δ 4.77 (2H, very br m, FWHM = 269.9 Hz, Tp-B**H**), 5.74 (6H, t, $^3J_{H-H}$ = 2.1 Hz, Tp-C^4**H**), 6.59 (1H, t, $^3J_{H-H}$ = 1.6 Hz, pz-C^4**H**), 6.88 (6H, d, $^3J_{H-H}$ = 1.8 Hz, Tp-C^3**H**), 7.42 (6H, dd, $^3J_{H-H}$ = 2.2 Hz, $^4J_{H-H}$ = 0.6 Hz, Tp-C^5**H**), 7.70 (2H, d, $^3J_{H-H}$ = 1.6 Hz, pz-C^3**H** and pz-C^5**H**) ppm; ^{11}B NMR (d_6-benzene): δ −2.86 (d, $^1J_{B-H}$ = 84.9 Hz, Tp-**B**) ppm; ^{11}B{^{1}H} NMR (d_6-benzene): δ −2.82 (s, Tp-**B**) ppm.

Reaction of 1-Sm(DME) and [Ln(Tp)$_2$(N″)] (Ln = Y, Sm) with carbon dioxide (CO_2) gas

General carbon dioxide (CO_2) gas reaction protocol. In the glovebox, a JY NMR tube was charged with the respective Ln-reagent powder, dissolved/suspended in deuterated solvent (0.5 mL), and cycled out. The JY NMR tube was cycled (x3) onto a Schlenk line *via* utilising a three-way tap connected separately to the JY NMR tube, the Schlenk line, and the outlet for the carbon dioxide (CO_2) gas. After final cycling of the system, the JY NMR tube was partially evacuated and then sealed. Then the entire system was evacuated and then sealed under static vacuum (10^{-2} mbar). The CO_2 gas was passed through a round-bottomed flask immersed in a dry-ice 2-propanol bath (−78 °C) and was used to pressurise the system (0.5 bar). The JY NMR tube tap was gently opened, and the Ln-solution/suspension exposed to the dry CO_2 atmosphere for a duration of 1 minute and then sealed. The reaction mixtures were then analysed by multinuclear NMR as quickly as possible.

Reaction of 1-Sm(DME) with CO_2 in d_8-THF and isolation of [{Sm(Tp)$_2$}$_2$(μ-η^2:η^2-O$_2$CCO$_2$)] 2-Sm. Reaction of a dark red-brown d_8-THF suspension of [Sm(Tp)$_2$(DME)] **1-Sm(DME)** (17.9 mg, 0.027 mmol) with CO_2 resulted in immediate decolourisation to yield a white suspension. d_8-THF (0.5 mL) was removed *in vacuo* from the suspension to yield pale cream

solids, which were dried *in vacuo* (10^{-2} mbar, 1 h) yielding dimeric $[\{Sm(Tp)_2\}_2(\mu\text{-}\eta^2\text{:}\eta^2\text{-}O_2CCO_2)]$ **2-Sm** (15.3 mg, 0.012 mmol, 92%). Complex **2-Sm** has extremely poor solubility in all solvents, therefore redissolving **2-Sm** after synthesis was unsuccessful. Due to the insolubility of **2-Sm** post-work-up, the NMR data obtained are from the NMR-scale reaction of **1-Sm(DME)** with CO_2 in d_8-THF. Block-shaped colourless single-crystals of **2-Sm** suitable for X-ray diffraction were grown directly from a saturated d_8-THF solution with a hexane anti-solvent at −35 °C over four months. ^{1}H NMR (d_8-THF): δ 4.87 (6H, s, Tp-C$^{3/5}$**H**), 6.04 (6H, approx. t, $^3J_{H-H}$ = 1.7 Hz, Tp-C^4**H**), 8.84 (6H, d, $^3J_{H-H}$ = 2.1 Hz, Tp-C$^{3/5}$**H**) ppm (Note: Tp-B**H** resonance was not observed in the ^{1}H NMR of **2-Sm**); ^{13}C{^{1}H} NMR (d_8-THF): δ 104.5 (s, Tp-**C**^{4}), 136.9 (s, Tp-**C**$^{3/5}$), 141.7 (s, Tp-**C**$^{3/5}$) ppm (Note: $\mathbf{C_2O_4}^{2-}$ resonance was not observed in the ^{13}C{^{1}H} NMR spectrum of **2-Sm**); ^{11}B NMR (d_8-THF): δ 2.91 (s, Tp-**B**) ppm; ^{11}B{^{1}H} NMR (d_8-THF): δ 2.91 (s, Tp-**B**) ppm. Anal. Calcd for $C_{38}H_{40}B_4N_{24}O_4Sm_2$: C, 36.78%; H, 3.25%; N, 27.09%. Found: C, 35.08%; H, 2.84%; N, 24.32%. IR (ATR): 3143 (w, $\upsilon_{sp^2\text{-}CH}$), 3116 (w, $\upsilon_{sp^2\text{-}CH}$), 2928 (w), 2857 (w), 2443 (w, υ_{BH}), 2408 (w, υ_{BH}), 2362 (w, υ_{BH}), 1649 (w, $\upsilon_{C=O}$), 1505 (m, $\upsilon_{C=C}$), 1431 (w), 1424 (w), 1404 (m), 1383 (m), 1294 (s), 1213 (s), 1198 (m), 1186 (m), 1120 (s), 1062 (m), 1045 (s), 1007 (m), 974 (s), 924 (w), 901 (w), 878 (w), 854 (w), 839 (w), 805 (w), 778 (m), 768 (s), 750 (s), 740 (s), 724 (s), 669 (s), 620 (m), 549 (w) cm^{-1}.

Reaction of [Y(Tp)$_2$(N″)] with CO$_2$ in d_6-benzene and isolation of [Y(Tp)$_2$(OSiMe$_3$)] 3-Y. Reaction of a colourless d_6-benzene solution of [Y(Tp)$_2$(N″)] (21.5 mg, 0.032 mmol) with CO_2 resulted in no colour or other observable changes. d_6-benzene (0.5 mL) and dissolved O=C=NSiMe$_3$ were removed *in vacuo* from the colourless solution to yield a colourless oil. Hexane (1 mL) was added to precipitate white solids, which were washed with hexane (1 mL) and the washing subsequently decanted away to remove impurities. All solvents were removed *in vacuo* and the resultant white powder was scraped with a spatula and dried *in vacuo* (10^{-2} mbar, 1 h) yielding [Y(Tp)$_2$(OSiMe$_3$)] **3-Y** (11.3 mg, 0.019 mmol, 59%). Complex **3-Y** has excellent solubility in toluene and moderate solubility in hexane. Rod-shaped colourless single-crystals of **3-Y** suitable for X-ray diffraction were grown from a saturated d_6-benzene solution with a hexane antisolvent at −35 °C overnight. ^{1}H NMR (d_6-benzene): δ −0.06 (9H, s, OSi(C**H**$_3$)$_3$), 4.82 (2H, very br m, FWHM = 228.1 Hz, Tp-B**H**), 5.81 (6H, t, $^3J_{H-H}$ = 2.1 Hz, Tp-C^4**H**), 7.26 (6H, d, $^3J_{H-H}$ = 1.4 Hz, Tp-C^3**H**), 7.49 (6H, d, $^3J_{H-H}$ = 2.1 Hz, Tp-C^5**H**) ppm; ^{13}C{^{1}H} NMR (d_6-benzene): δ 3.2 (s, OSi(**C**H$_3$)$_3$), 104.5 (s, Tp-**C**^{4}), 135.2 (s, Tp-**C**^{5}) 142.0 (s, Tp-**C**^{3}) ppm; ^{11}B NMR (d_6-benzene): δ −2.93 (d, $^1J_{B-H}$ = 44.8 Hz, Tp-**B**) ppm; ^{11}B{^{1}H} NMR (d_6-benzene): δ −2.72 (s, Tp-**B**) ppm. Anal. Calcd for $C_{21}H_{29}B_2N_{12}OSiY$: C, 41.75%; H, 4.84%; N, 27.82%. Found: C, 36.68%; H, 3.08%; N, 24.81%. Lower CHN values than calculated are the result of minor byproducts that could not be eliminated by recrystallisation of **3-Y**. IR (ATR): 3616 (w), 3139 (w, $\upsilon_{sp^2\text{-}CH}$), 2947 (w, $\upsilon_{sp^3\text{-}CH}$), 2456 (w, υ_{BH}), 2416 (w, υ_{BH}), 2373 (w, υ_{BH}), 1720 (w), 1504 (m, $\upsilon_{C=C}$), 1404 (m), 1387 (m), 1299 (s), 1252 (w), 1240 (w), 1214 (s), 1200 (m), 1187 (m), 1120 (s), 1065 (w), 1046 (s), 975 (s), 950 (s), 924 (w), 887 (2), 824 (w), 781 (m), 737 (s), 722 (s), 670 (s), 621 (s) cm^{-1}.

Reaction of [Sm(Tp)$_2$(N″)] with CO$_2$ in d_6-benzene and isolation of [Sm(Tp)$_2$(OSiMe$_3$)] 3-Sm. Reaction of a white d_6-benzene suspension of [Sm(Tp)$_2$(N″)] (18.5 mg, 0.025 mmol) with CO_2 resulted in no colour or other observable changes. d_6-benzene (0.5 mL) and dissolved O=C=NSiMe$_3$ were removed *in vacuo* from the white suspension to yield a colourless oil. Hexane (1 mL) was added to precipitate white solids, which were washed with hexane (1 mL) and the washing subsequently decanted away to remove impurities. All solvents were removed *in vacuo* and the resultant white powder was scraped with a spatula and dried *in vacuo* (10^{-2} mbar, 1 h) yielding [Sm(Tp)$_2$(OSiMe$_3$)] **3-Sm** (8.8 mg, 0.013 mmol, 53%). Complex **3-Sm** has excellent solubility in toluene and moderate solubility in hexane. Tablet-shaped colourless single-crystals of **3-Sm** suitable for X-ray diffraction were grown from a saturated hexane solution at −35 °C over three months. ^{1}H NMR (d_6-benzene): δ 2.56 (9H, s, overlapped with the resonance at δ 2.61 ppm integrating to 6H, FWHM = 16.1 Hz, OSi(C**H**$_3$)$_3$), 2.61 (6H, br s, overlapped with the resonance at δ 2.56 ppm integrating to 9H, FWHM = 26.3 Hz, Tp-C^4**H**), 5.64 (6H, d, $^3J_{H-H}$ = 1.8 Hz, Tp-C$^{3/5}$**H**), 8.22 (2H, very br m, FWHM = 283.8 Hz, Tp-B**H**), 8.96 (6H, d, $^3J_{H-H}$ = 1.9 Hz, Tp-C$^{3/5}$**H**) ppm; ^{13}C{^{1}H} NMR (d_6-benzene): δ 6.0 (s, OSi(**C**H$_3$)$_3$), 103.4 (s, Tp-**C**$^{3/5}$), 136.3 (s, Tp-**C**$^{3/5}$), 139.9 (s, Tp-**C**^{4}) ppm; ^{11}B NMR (d_6-benzene): δ 5.43 (d, $^1J_{B-H}$ = 76.5 Hz, Tp-**B**) ppm; ^{11}B{^{1}H} NMR (d_6-benzene): δ 5.43 (s, Tp-**B**) ppm. Anal. Calcd for $C_{21}H_{29}B_2N_{12}OSiSm$: C, 37.89%; H, 4.39%; N, 25.25%. Found: C, 39.00%; H, 3.83%; N, 23.65%. IR (ATR): 3626 (w), 3146 (w, $\upsilon_{sp^2\text{-}CH}$), 2949 (w, $\upsilon_{sp^3\text{-}CH}$), 2893 (w, $\upsilon_{sp^3\text{-}CH}$), 2452 (w, υ_{BH}), 2412 (w, υ_{BH}), 2367 (w, υ_{BH}), 1503 (m, $\upsilon_{C=C}$), 1403 (m), 1383 (m), 1297 (s), 1254 (w), 1240 (w), 1212 (s), 1198 (m), 1187 (m), 1118 (s), 1065 (m), 1044 (s), 974 (s), 956 (s), 924 (w), 825 (m), 805 (w), 760 (s), 738 (s), 721 (s), 670 (s), 621 (s) cm^{-1}.

Isolation of cluster [Sm$_5$(Tp)$_6$(μ_2-OH)$_6$(μ_3-OH)$_2$(μ_4-OH)] 4-Sm in the adventitious moisture-mediated decomposition of [Sm(Tp)$_2$(N″)]

On one occasion a toluene solution of [Sm(Tp)$_2$(N″)] reacted with adventitious moisture in the solvent yielding [Sm$_5$(Tp)$_6$(μ_2-OH)$_6$(μ_3-OH)$_2$(μ_4-OH)] **4-Sm**. Plate-shaped colourless single-crystals of **4-Sm** suitable for X-ray diffraction were grown from a dilute hexane solution at −35 °C over a week. ^{1}H NMR (d_6-benzene): δ −1.47 (9H under integrating as 3H, br s, FWHM = 21.4 Hz, μ-O**H**), 5.14 (18H, very br s, overlapped with the resonance at δ 5.71 ppm integrating to 18H, FWHM = 282.0 Hz, Tp-C**H**), 5.71 (18H, br s, overlapped with the resonance at δ 5.14 ppm integrating to 18H, FWHM = 26.4 Hz, Tp-C**H**), 6.79 (6H, overlapped with the d_6-benzene resonance, FWHM = 329.2 Hz, Tp-B**H**), 8.40 (18H, s, FWHM = 10.4 Hz, Tp-C**H**) ppm; ^{13}C{^{1}H} NMR (d_6-benzene): δ 103.6 (s, Tp-**C**), 135.3 (s, Tp-**C**), 141.2 (br s, Tp-**C**) ppm; ^{11}B NMR (d_6-benzene): δ 1.55 (d, $^1J_{B-H}$ = 39.5 Hz, Tp-**B**) ppm; ^{11}B{^{1}H} NMR (d_6-benzene): δ 1.36 (s, Tp-**B**) ppm. IR (ATR): 3146 (w, $\upsilon_{sp^2\text{-}CH}$), 3118 (w, $\upsilon_{sp^2\text{-}CH}$), 2441 (w, υ_{BH}), 2409 (w, υ_{BH}), 2374 (w, υ_{BH}), 1505 (m, $\upsilon_{C=C}$),

1431 (w), 1423 (w), 1402 (m), 1383 (m), 1295 (s), 1212 (s), 1198 (m), 1186 (m), 1119 (s), 1062 (m), 1045 (s), 974 (m), 923 (w), 900 (w), 879 (w), 806 (w), 778 (m), 768 (s), 750 (s), 739 (m), 723 (s), 669 (m), 620 (m) cm^{-1}.

Conflicts of interest

There are no conflicts to declare.

Acknowledgements

We acknowledge the University of Glasgow (UoG) for funding, and the award of a College of Science and Engineering (UoG) PhD Scholarship to T. C. We thank Dr Zeliha Ertekin from the research group of Professor Dr Mark D. Symes (UoG) for lending us a carbon dioxide gas cylinder. We are grateful to Professor Dr Peter W. Roesky at the Karlsruhe Institute of Technology (KIT, Germany) for valuable discussions on reactivity of Sm(II) and Mr David Frick for investigating the reactivity of Ln(II) **1-Sm(DME)** and [Yb(Tp)$_2$] with pnictogens (P_4, $As^0{}_{nano}$) at KIT. We thank the EPSRC UK National Crystallography Service at the University of Southampton for the collection of the crystallographic data for **2-Sm** and **4-Sm** and additionally Diamond Light Source for an award of beamtime on I19 (CY31778) for **2-Sm**.

References

1 (*a*) K. A. Grice, *Coord. Chem. Rev.*, 2017, **336**, 78–95; (*b*) K. Blaziak, D. Tzeli, S. S. Xantheas and E. Uggerud, *Phys. Chem. Chem. Phys.*, 2018, **20**, 25495–25505.

2 (*a*) U. Bayer and R. Anwander, *Dalton Trans.*, 2020, **49**, 17472–17493; (*b*) O. P. Lam and K. Meyer, *Polyhedron*, 2012, **32**, 1–9.

3 M. Pérez-Jiménez, H. Corona, F. de la Cruz-Martínez and J. Campos, *Chem. – Eur. J.*, 2023, **29**, e202301428.

4 (*a*) D. H. Gibson, *Chem. Rev.*, 1996, **96**, 2063–2096; (*b*) A. Paparo and J. Okuda, *Coord. Chem. Rev.*, 2017, **334**, 136–149.

5 Q. Liu, L. Wu, R. Jackstell and M. Beller, *Nat. Commun.*, 2015, **6**, 5933.

6 (*a*) J. C. Wedal and W. J. Evans, *J. Am. Chem. Soc.*, 2021, **143**, 18354–18367; (*b*) M. Szostak and D. J. Procter, *Angew. Chem., Int. Ed.*, 2012, **51**, 9238–9256.

7 (*a*) W. J. Evans, C. A. Seibel and J. W. Ziller, *Inorg. Chem.*, 1998, **37**, 770–776; (*b*) W. J. Evans, J. M. Perotti, J. C. Brady and J. W. Ziller, *J. Am. Chem. Soc.*, 2003, **125**, 5204–5212; (*c*) L. Castro, S. Labouille, D. R. Kindra, J. W. Ziller, F. Nief, W. J. Evans and L. Maron, *Chem. – Eur. J.*, 2012, **18**, 7886–7895; (*d*) L. Castro, D. P. Mills, C. Jones and L. Maron, *Eur. J. Inorg. Chem.*, 2016, **2016**, 792–796; (*e*) H. M. Nicholas and D. P. Mills, *Encyclopedia of Inorganic and Bioinorganic Chemistry*, 2017, 1–10. DOI: 10.1002/9781119951438.eibc2453; (*f*) M. Xémard, V. Goudy, A. Braun, M. Tricoire, M. Cordier, L. Ricard, L. Castro, E. Louyriac, C. E. Kefalidis, C. Clavaguéra, L. Maron and G. Nocton, *Organometallics*, 2017, **36**, 4660–4668; (*g*) M. Xémard, M. Cordier, E. Louyriac, L. Maron, C. Clavaguéra and G. Nocton, *Dalton Trans.*, 2018, **47**, 9226–9230; (*h*) N. W. Davies, A. S. P. Frey, M. G. Gardiner and J. Wang, *Chem. Commun.*, 2006, 4853–4855, DOI: 10.1039/B611784H.

8 N. Tsoureas, L. Castro, A. F. R. Kilpatrick, F. G. N. Cloke and L. Maron, *Chem. Sci.*, 2014, **5**, 3777–3788.

9 C. J. Inman, A. S. P. Frey, A. F. R. Kilpatrick, F. G. N. Cloke and S. M. Roe, *Organometallics*, 2017, **36**, 4539–4545.

10 (*a*) J. Zhang and X. Zhou, *Dalton Trans.*, 2011, **40**, 9637–9648; (*b*) H. Yin, P. J. Carroll and E. J. Schelter, *Chem. Commun.*, 2016, **52**, 9813–9816; (*c*) W. J. Evans, C. H. Fujimoto and J. W. Ziller, *Organometallics*, 2001, **20**, 4529–4536.

11 (*a*) R. D. Dicken, A. Motta and T. J. Marks, *ACS Catal.*, 2021, **11**, 2715–2734; (*b*) R. Anwander, in *Organolanthoid Chemistry: Synthesis, Structure, Catalysis*, Springer Berlin Heidelberg, Berlin, Heidelberg, 1996, pp. 33–112. DOI: 10.1007/BFb0015595.

12 (*a*) E. C. Alyea, D. C. Bradley and R. G. Copperthwaite, *J. Chem. Soc., Dalton Trans.*, 1972, 1580–1584, DOI: 10.1039/dt9720001580; (*b*) D. C. Bradley, J. S. Ghotra and F. A. Hart, *J. Chem. Soc., Dalton Trans.*, 1973, 1021–1023, DOI: 10.1039/dt9730001021; (*c*) P. G. Eller, D. C. Bradley, M. B. Hursthouse and D. W. Meek, *Coord. Chem. Rev.*, 1977, **24**, 1–95; (*d*) C. A. P. Goodwin and D. P. Mills, in *Organometallic Chemistry*, ed. I. Fairlamb, J. M. Lynam, N. J. Patmore and P. Elliott, The Royal Society of Chemistry, 2017, vol. 41.

13 (*a*) Z. R. Turner, *Inorganics*, 2015, **3**, 597–635; (*b*) M. G. Gardiner and D. N. Stringer, *Materials*, 2010, **3**, 841–862.

14 (*a*) M. N. Bochkarev, E. A. Fedorova, Y. F. Radkov, S. Y. Khorshev, G. S. Kalinina and G. A. Razuvaev, *J. Organomet. Chem.*, 1983, **258**, C29–C33; (*b*) C. Krempner and B. McNerney, in *Encyclopedia of Inorganic and Bioinorganic Chemistry*, 2012, DOI: 10.1002/9781119951438.eibc2089.

15 L. R. Sita, J. R. Babcock and R. Xi, *J. Am. Chem. Soc.*, 1996, **118**, 10912–10913.

16 T. J. Boyle and L. A. M. Ottley, *Chem. Rev.*, 2008, **108**, 1896–1917.

17 (*a*) J. Takats, *J. Alloys Compd.*, 1997, **249**, 52–55; (*b*) A. C. Hillier, S. Y. Liu, A. Sella and M. R. J. Elsegood, *J. Alloys Compd.*, 2000, **303–304**, 83–93; (*c*) N. Marques, A. Sella and J. Takats, *Chem. Rev.*, 2002, **102**, 2137–2160; (*d*) C. Hossack, C. Cahill and C. Besson, *Dalton Trans.*, 2023, **52**, 17656–17665.

18 A. C. Hillier, A. Sella and M. R. J. Elsegood, *J. Organomet. Chem.*, 2002, **664**, 298–305.

19 G. H. Maunder, M. R. Russo and A. Sella, *Polyhedron*, 2004, **23**, 2709–2714.

20 X. Zhang, G. R. Loppnow, R. McDonald and J. Takats, *J. Am. Chem. Soc.*, 1995, **117**, 7828–7829.

21 M. Kühling, R. McDonald, P. Liebing, L. Hilfert, M. J. Ferguson, J. Takats and F. T. Edelmann, *Dalton Trans.*, 2016, **45**, 10118–10121.
22 (*a*) A. C. Hillier, S.-Y. Liu, A. Sella and M. R. J. Elsegood, *Inorg. Chem.*, 2000, **39**, 2635–2644; (*b*) I. Lopes, A. C. Hillier, S. Y. Liu, Â. Domingos, J. Ascenso, A. Galvão, A. Sella and N. Marques, *Inorg. Chem.*, 2001, **40**, 1116–1125.
23 J. Takats, X. W. Zhang, V. W. Day and T. A. Eberspacher, *Organometallics*, 1993, **12**, 4286–4288.
24 I. Lopes, R. Dias, Â. Domingos and N. Marques, *J. Alloys Compd.*, 2002, **344**, 60–64.
25 Â. Domingos, I. Lopes, J. C. Waerenborgh, N. Marques, G. Y. Lin, X. W. Zhang, J. Takats, R. McDonald, A. C. Hillier, A. Sella, M. R. J. Elsegood and V. W. Day, *Inorg. Chem.*, 2007, **46**, 9415–9424.
26 I. Lopes, G. Y. Lin, A. Domingos, R. McDonald, N. Marques and J. Takats, *J. Am. Chem. Soc.*, 1999, **121**, 8110–8111.
27 G. Lin, R. McDonald and J. Takats, *Organometallics*, 2000, **19**, 1814–1816.
28 (*a*) A. C. Hillier, S. Y. Liu, A. Sella, O. Zekria and M. R. J. Elsegood, *J. Organomet. Chem.*, 1997, **528**, 209–215; (*b*) A. C. Hillier, A. Sella and M. R. J. Elsegood, *J. Organomet. Chem.*, 1999, **588**, 200–204.
29 A. C. Hillier, X. W. Zhang, G. H. Maunder, S. Y. Liu, T. A. Eberspacher, M. V. Metz, R. McDonald, Â. Domingos, N. Marques, V. W. Day, A. Sella and J. Takats, *Inorg. Chem.*, 2001, **40**, 5106–5116.
30 (*a*) M. A. J. Moss, R. A. Kresinski, C. J. Jones and W. J. Evans, *Polyhedron*, 1993, **12**, 1953–1955; (*b*) Â. Domingos, J. Marçalo, N. Marques, A. P. D. Matos, A. Galvão, P. C. Isolani, G. Vicentini and K. Zinner, *Polyhedron*, 1995, **14**, 3067–3076; (*c*) X. Zhang, R. McDonald and J. Takats, *New J. Chem.*, 1995, **19**, 573–585; (*d*) K. O. Saliu, J. Takats and M. J. Ferguson, *Acta Crystallogr., Sect. E: Struct. Rep. Online*, 2009, **65**, m643–m644; (*e*) A. Momin, L. Carter, Y. Yang, R. McDonald, S. Essafi, F. Nief, I. Del Rosal, A. Sella, L. Maron and J. Takats, *Inorg. Chem.*, 2014, **53**, 12066–12075; (*f*) M. Kühling, C. Wickleder, M. J. Ferguson, C. G. Hrib, R. McDonald, M. Suta, L. Hilfert, J. Takats and F. T. Edelmann, *New J. Chem.*, 2015, **39**, 7617–7625.
31 T. Chowdhury, M. J. Evans, M. P. Coles, A. G. Bailey, W. J. Peveler, C. Wilson and J. H. Farnaby, *Chem. Commun.*, 2023, **59**, 2134–2137.
32 (*a*) T. Chowdhury, S. J. Horsewill, C. Wilson and J. H. Farnaby, *Aust. J. Chem.*, 2022, **75**, 660–675; (*b*) T. Chowdhury, C. Wilson, C. Maichle-Mössmer, R. Anwander and J. H. Farnaby, *Eur. J. Inorg. Chem.*, 2024, **27**, e202300731; (*c*) T. Chowdhury, F. Murphy, A. R. Kennedy, C. Wilson, J. H. Farnaby and C. E. Weetman, *Inorg. Chem.*, 2024, **63**, 9390–9394.
33 J. L. Galler, S. Goodchild, J. Gould, R. McDonald and A. Sella, *Polyhedron*, 2004, **23**, 253–262.
34 (*a*) L. J. Nugent, R. D. Baybarz, J. L. Burnett and J. L. Ryan, *J. Phys. Chem.*, 1973, **77**, 1528–1539; (*b*) L. R. Morss, *Chem. Rev.*, 1976, **76**, 827–841.
35 (*a*) F. Nief, *Dalton Trans.*, 2010, **39**, 6589; (*b*) D. H. Woen and W. J. Evans, in *Handbook on the Physics and Chemistry of Rare Earths*, ed. J.-C. G. Bünzli and V. K. Pecharsky, Elsevier, 2016, vol. 50, pp. 337–394.
36 (*a*) M. V. R. Stainer and J. Takats, *J. Am. Chem. Soc.*, 1983, **105**, 410–415; (*b*) C. Apostolidis, J. Rebizant, B. Kanellakopulos, R. Von Ammon, E. Dornberger, J. Müller, B. Powietzka and B. Nuber, *Polyhedron*, 1997, **16**, 1057–1068; (*c*) I. Lopes, B. Monteiro, G. Lin, Â. Domingos, N. Marques and J. Takats, *J. Organomet. Chem.*, 2001, **632**, 119–125.
37 (*a*) J. H. Farnaby, F. G. N. Cloke, M. P. Coles, J. C. Green and G. Aitken, *C. R. Chim.*, 2010, **13**, 812–820; (*b*) F. Ortu, H. Zhu, M.-E. Boulon and D. Mills, *Inorganics*, 2015, **3**, 534–553.
38 (*a*) R. D. Shannon, *Acta Crystallogr., Sect. A: Cryst. Phys., Diffr., Theor. Gen. Crystallogr.*, 1976, **32**, 751–767; (*b*) R. E. Cramer, J. M. Rimsza and T. J. Boyle, *Inorg. Chem.*, 2022, **61**, 6120–6127.
39 (*a*) S. J. Swamy, J. Loebel, J. Pickardt and H. Schumann, *J. Organomet. Chem.*, 1988, **353**, 27–34; (*b*) M. Håkansson, M. Vestergren, B. Gustafsson and G. Hilmersson, *Angew. Chem., Int. Ed.*, 1999, **38**, 2199–2201.
40 S. N. Konchenko, N. A. Pushkarevsky, M. T. Gamer, R. Köppe, H. Schnöckel and P. W. Roesky, *J. Am. Chem. Soc.*, 2009, **131**, 5740–5741.
41 (*a*) H. Reddmann, C. Apostolidis, O. Walter, J. Rebizant and H.-D. Amberger, *Z. Anorg. Allg. Chem.*, 2005, **631**, 1487–1496; (*b*) C. Apostolidis, A. Kovács, A. Morgenstern, J. Rebizant and O. Walter, *Inorganics*, 2021, **9**, 44.
42 C. Schoo, S. Bestgen, A. Egeberg, J. Seibert, S. N. Konchenko, C. Feldmann and P. W. Roesky, *Angew. Chem., Int. Ed.*, 2019, **58**, 4386–4389.
43 M. A. J. Moss and C. J. Jones, *Polyhedron*, 1989, **8**, 2367–2370.
44 T. I. Gountchev and T. D. Tilley, *Organometallics*, 1999, **18**, 2896–2905.
45 Y. Ma, Y.-Q. Zhai, Y.-S. Ding, T. Han and Y.-Z. Zheng, *Chem. Commun.*, 2020, **56**, 3979–3982.
46 M. Karl, G. Seybert, W. Massa, K. Harms, S. Agarwal, R. Maleika, W. Stelter, A. Greiner, W. H. B. Neumüller and K. Dehnicke, *Z. Anorg. Allg. Chem.*, 1999, **625**, 1301–1309.
47 (*a*) A. Mortis, C. Maichle-Mössmer and R. Anwander, *Dalton Trans.*, 2022, **51**, 1070–1085; (*b*) G. Lapadula, A. Bourdolle, F. Allouche, M. P. Conley, I. del Rosal, L. Maron, W. W. Lukens, Y. Guyot, C. Andraud, S. Brasselet, C. Copéret, O. Maury and R. A. Andersen, *Chem. Mater.*, 2014, **26**, 1062–1073.
48 (*a*) M. J. McGeary, P. S. Coan, K. Folting, W. E. Streib and K. G. Caulton, *Inorg. Chem.*, 1989, **28**, 3283–3284; (*b*) P. S. Gradeff, K. Yunlu, T. J. Deming, J. M. Olofson, R. J. Doedens and W. J. Evans, *Inorg. Chem.*, 1990, **29**, 420–424; (*c*) M. J. McGeary, P. S. Coan, K. Folting, W. E. Streib and K. G. Caulton, *Inorg. Chem.*, 1991, **30**, 1723–1735.
49 T. J. Boyle, F. Guerrero, R. E. Cramer, P. C. Reuel, D. M. Boye and H. L. Brooks, *Inorg. Chem.*, 2022, **61**, 5048–5059.
50 Z. Xie, K. Chui, Q. Yang, T. C. W. Mak and J. Sun, *Organometallics*, 1998, **17**, 3937–3944.